Supporting Information

Ternary polymer solar cells: Impact of non-fullerene acceptors on optical and morphological properties

Quentin Eynaud,[1] Tomoyuki Koganezawa,[2] Hidehiro Sekimoto,[3] Mohamed el Amine Kramdi,[1] Gilles Quéléver,[1] Olivier Margeat,[1] Jörg Ackermann[1], Noriyuki Yoshimoto[3] and Christine Videlot-Ackermann [1,*]

[1] Aix Marseille Univ., CNRS, CINaM, Marseille, France
[2] Industrial Application Division, Japan Synchrotron Radiation Research Institute (JASRI), Sayo, Hyogo 679-5198, Japan
[3] Department of Physical Science and Materials Engineering, Iwate University, Ueda Morioka 020 8551, Japan
[*] Correspondence: christine.videlot-ackermann@cnrs.fr

Chemical name of donor material:

P3HT   poly(3-hexylthiophene-2,5-diyl)

Chemical name of acceptor materials:

$PC_{61}BM$ [6,6]-phenyl-C61-butyric-acid-methyl ester

ITIC   3,9-bis(2-methylene-(3-(1,1-dicyanomethylene)-indanone))-5,5,11,11-tetrakis(4-hexylphenyl)-dithieno[2,3-d:2',3'-d']-s-indaceno[1,2-b:5,6-b']dithiophene

eh-IDTBR   (5Z)-3-ethyl-2-sulfanylidene-5-   [[4-[9,9,18,18-tetrakis(2-ethylhexyl)-15-[7-[(Z)-(3-ethyl-4-oxo-2-sulfanylidene-1,3-thiazolidin-5-ylidene)methyl]-2,1,3-benzothiadiazol-4-yl]-5,14-dithiapentacyclo[10.6.0.0^{3,10}.0^{4,8}.0^{13,17}]octadeca-1(12),2,4(8),6,10,13(17),15-heptaen-6-yl]-2,1,3-benzothiadiazol-7-yl]methylidene]-1,3-thiazolidin-4-one
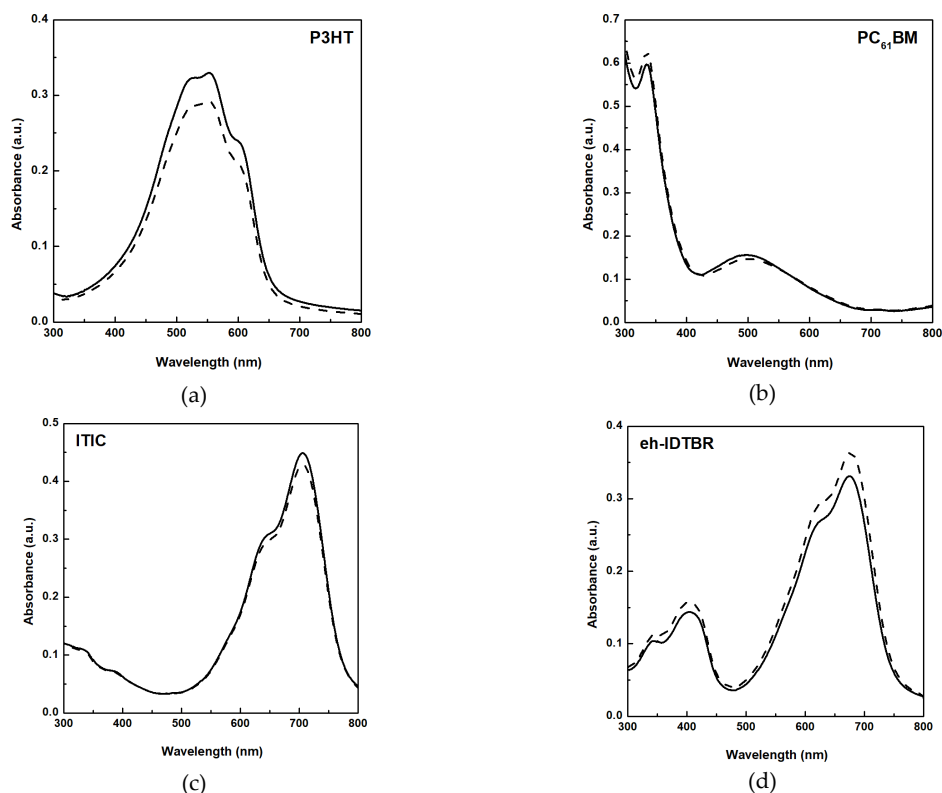
Figure S1: Absorption spectra of neat films depending on annealing temperature (100°C in dotted line and 140°C in solid-line): P3HT (a), PC$_{61}$BM (b), ITIC (c) and eh-IDTBR (d).

Table S1: Intensity and wavelength of maximum absorption peaks (from Figure S1) for neat films of P3HT, PC$_{61}$BM, ITIC and eh-IDTBR.

	100°C		140°C		Abs.(140°C)/Abs.(100°C)
	Abs.	λ (nm)	Abs.	λ (nm)	
P3HT	0.29	552	0.33	552	1.13
PC$_{61}$BM	0.14	499	0.15	500	1.07
ITIC	0.43	706	0.44	706	1.02
eh-IDTBR	0.36	677	0.33	674	0.91

For eh-IDTBR, the absorption spectrum at 100°C is more intense than that at 140°C with Abs.(140°C)/Abs.(100°C)=0.91. This increase reflects a speicific change in the orientation of the molecules induced by thermal annealing. 2D-GIXRD measurements on eh-IDTBR films annealed at 100°C and 140°C provide explanations (Figure S7). At 100°C, the intense (010) diffraction peak in out-of-profile (q$_z$) strengthens the face-on orientation of eh-IDTBR molecules, which increases the surface area absorbing the photons, and consequently the absorption intensity in Figure S1d. At 140°C, the emergence of an intense, narrow diffraction peak indexed (100) and its replicas (200) and (300) in q$_z$ profile highlights a very significant change in the orientation of the molecules, from face-on orientation to edge-on, reducing the surface area for photon absorption. With a Abs.(140°C)/Abs.(100°C)=1.02, no significant impact of thermal annealing is observe for ITIC films.
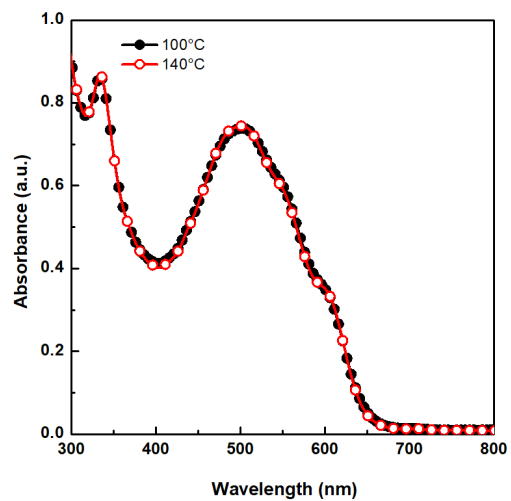
Figure S2: Absorption spectra of binary P3HT:$PC_{61}BM$ films depending on annealing temperature (100°C and 140°C). In these non-normalized spectra, the fullerene peak at 335 nm is unaffected by blend annealing, so the absorption spectra of ternary mixtures in Figures 2c and 2d can be normalized to this peak.

Table S2: Electron and hole mobility values determinate by SCLC protocol for electron-only and hole-only devices based on P3HT, P3HT:PC$_{61}$BM, P3HT:PC$_{61}$BM:ITIC and P3HT:PC$_{61}$BM:eh-IDTBR layers as function of thermal annealing temperature (100°C or 140°C). The thickness of each layer is indicated as required for the SCLC protocol. The average values ($\mu_{average}$) of the mobilities were taken to produce the Figure 7.

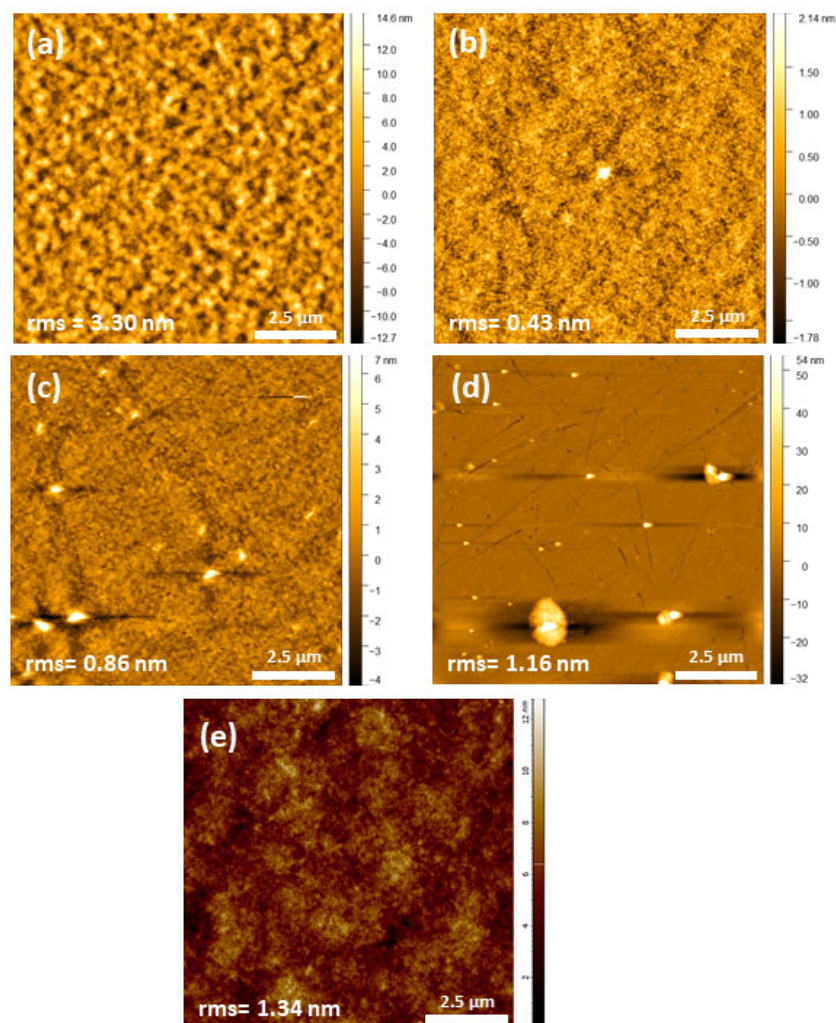|		**P3HT**		**P3HT:PC$_{61}$BM**		**P3HT:PC$_{61}$BM:ITIC**		**P3HT:PC$_{61}$BM:eh-IDTBR**	
electrons	Temperature			100°C	140°C	100°C	140°C	100°C	140°C
	Tickness (nm)			206	220	174	191	173	195
	$\mu_{average}$ (cm^2.V^{-1}.s^{-1})			$1.26.10^{-8}$	$1.27.10^{-5}$	$1.77.10^{-5}$	$1.99.10^{-4}$	$7.86.10^{-6}$	$4.13.10^{-4}$
	Standard deviation			$1.51.10^{-8}$	$1.25.10^{-5}$	$1.97.10^{-5}$	$9.09.10^{-5}$	$4.75.10^{-6}$	$1.10.10^{-4}$
	μ_{min} (cm^2.V^{-1}.s^{-1})			$1.03.10^{-10}$	$6.31.10^{-6}$	$2.41.10^{-6}$	$1.03.10^{-4}$	$1.71.10^{-6}$	$2.37.10^{-4}$
	μ_{max} (cm^2.V^{-1}.s^{-1})			$6.10.10^{-8}$	$7.75.10^{-5}$	$6.58.10^{-5}$	$3.76.10^{-4}$	$1.99.10^{-5}$	$6.13.10^{-4}$
holeless	Temperature (°C)	100°C	140°C	100°C	140°C	100°C	140°C	100°C	140°C
	Tickness (nm)	92	101	194	199	187	198	200	198
	$\mu_{average}$ (cm^2.V^{-1}.s^{-1})	$2.73.10^{-4}$	$2.35.10^{-4}$	$1.06.10^{-3}$	$2.17.10^{-3}$	$2.20.10^{-5}$	$5.14.10^{-3}$	$6.49.10^{-4}$	$6.43.10^{-3}$
	Standard deviation	$6.45.10^{-6}$	$5.90.10^{-6}$	$6.66.10^{-6}$	$4.86.10^{-5}$	$9.07.10^{-8}$	$2.05.10^{-5}$	$1.01.10^{-6}$	$3.38.10^{-5}$
	μ_{min} (cm^2.V^{-1}.s^{-1})	$1.43.10^{-4}$	$1.62.10^{-4}$	$9.06.10^{-4}$	$1.51.10^{-3}$	$1.58.10^{-5}$	$3.77.10^{-3}$	$4.93.10^{-4}$	$4.40.10^{-3}$
	μ_{max} (cm^2.V^{-1}.s^{-1})	$3.69.10^{-4}$	$3.15.10^{-4}$	$1.23.10^{-3}$	$3.02.10^{-3}$	$2.71.10^{-5}$	$6.49.10^{-3}$	$7.97.10^{-4}$	$8.04.10^{-3}$

Figure S3: AFM images of neat P3HT (a), $PC_{61}BM$ (b), ITIC (c), eh-IDTBR (d) films and ternary P3HT:$PC_{61}BM$:ITIC blend (e) thermal annealed at 140°C. Size of micrographies: 10 x 10 μm².
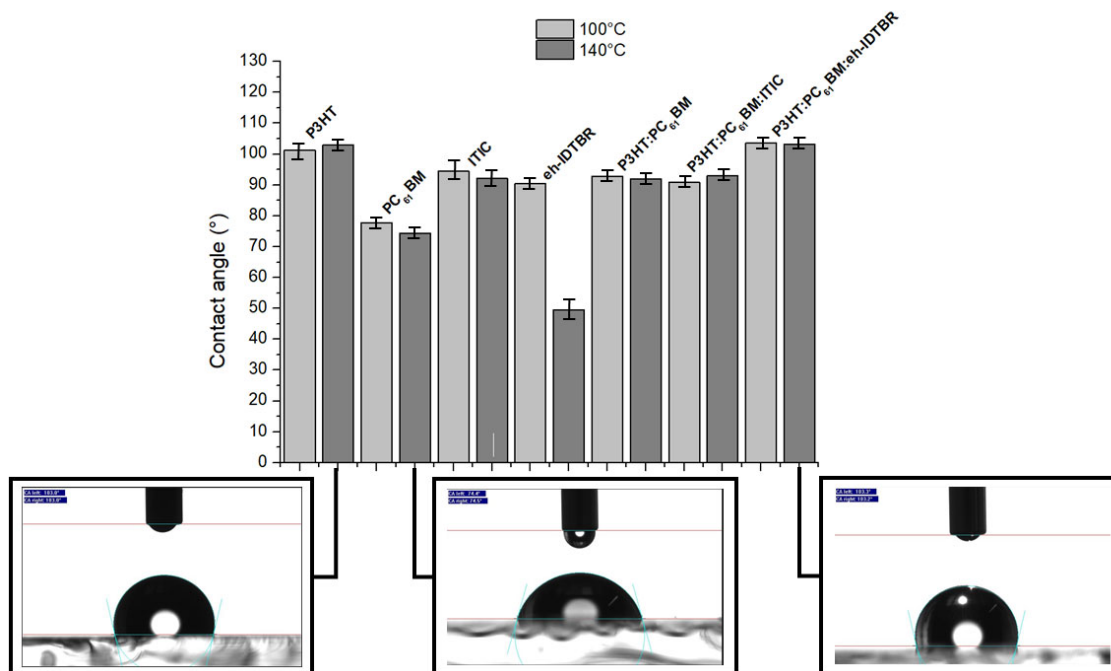
Figure S4: Graph showing water contact angle on neat films (P3HT, PC$_{61}$BM, ITIC and eh-IDTBR), binary (P3HT:PC$_{61}$BM) and ternary (P3HT:PC$_{61}$BM:ITIC and P3HT:PC$_{61}$BM:eh-IDTBR) blends as function of thermal annealing temperature (100°C and 140°C). Corresponding images for PH3T, PC$_{61}$BM and P3HT:PC$_{61}$BM:eh-IDTBR at 140°C.

When the substrate consists of two kinds of species, the Cassie-Baxter equation [1,2] obtains the form:

$$\cos\theta = f_1 \cos\theta_1 + f_2 \cos\theta_2$$

where θ is the WCA measured on the surface composed of the two compounds (compound 1 and compound 2), θ_1 is the WCA measured on the surface composed of compound 1 and θ_2 is the WCA measured on the surface composed of compound 2. f_1 and f_2 are the fraction of compound 1 and compound 2.
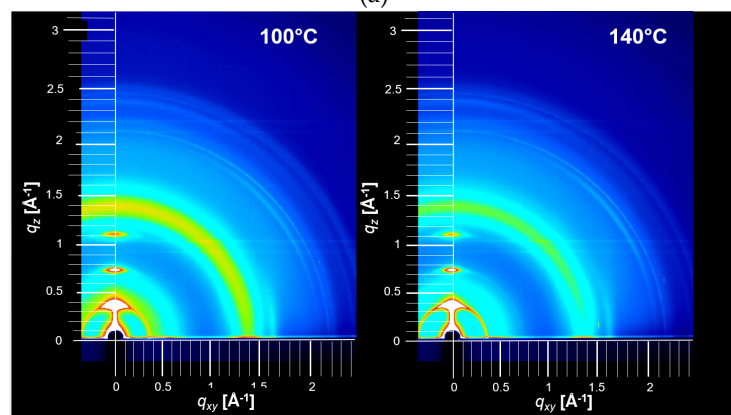
In the case of the binary P3HT:PC$_{61}$BM blend, f_{P3HT} and f_{PC61BM} are 0.48 and 0.52 at 100°C; and 0.88 and 0.12 at 140°C.

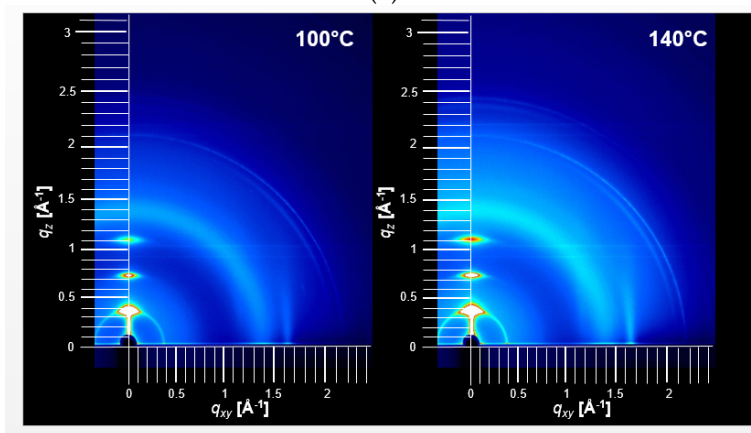[1] Cassie A. B. D.; Baxter S., Wettablity of porous surfaces, Trans. Faraday Soc. 1944, 40, 546 – 551.

[2] Cassie A. B. D. Contact angles, Discuss. Faraday Soc., 1948, 3, 11 – 16.
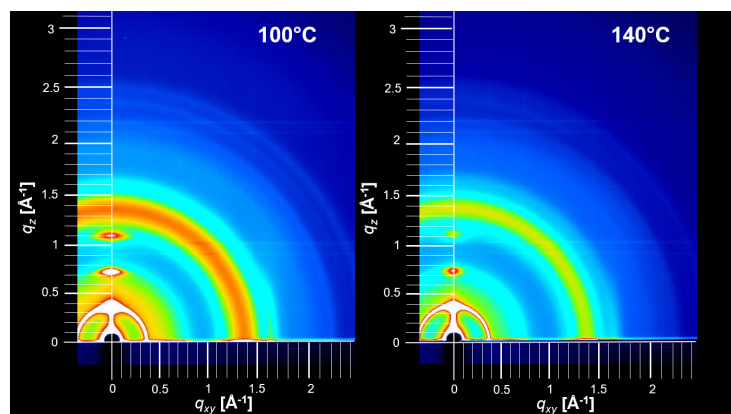
Figure S5: 2D-GIXRD patterns of P3HT:PC$_{61}$BM (a), P3HT:PC$_{61}$BM:ITIC (b) and P3HT:PC$_{61}$:eh-IDTBR (c) blends as function of thermal annealing temperature.
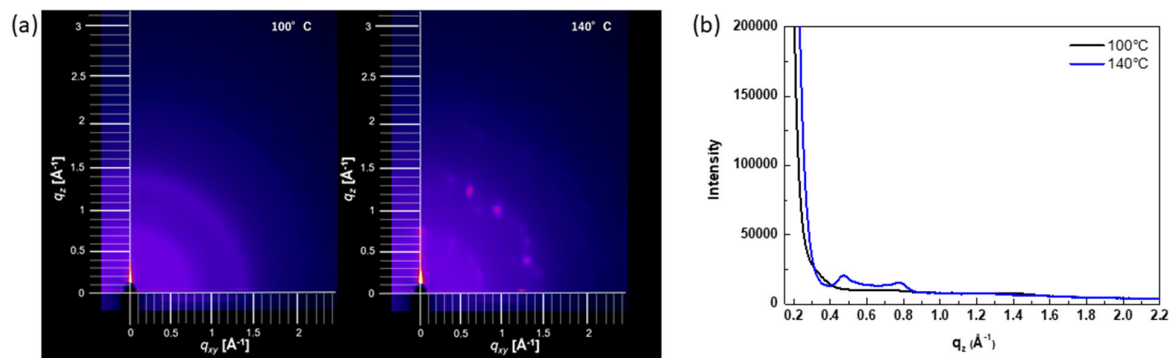
Figure S6: 2D-GIXRD patterns (a) and corresponding out of plane profiles (b) of PC$_{61}$BM layers as function of thermal annealing temperature.
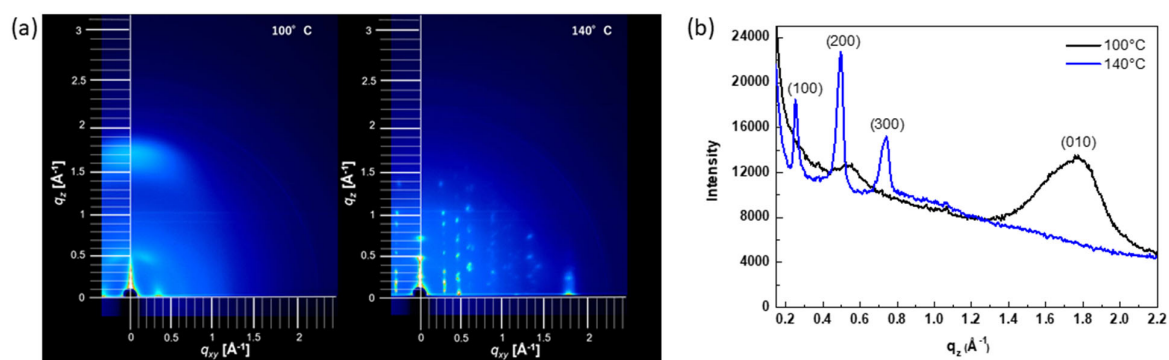

Figure S7: 2D-GIXRD patterns (a) and corresponding out of plane profiles (b) of eh-IDTBR layers as function of thermal annealing temperature.
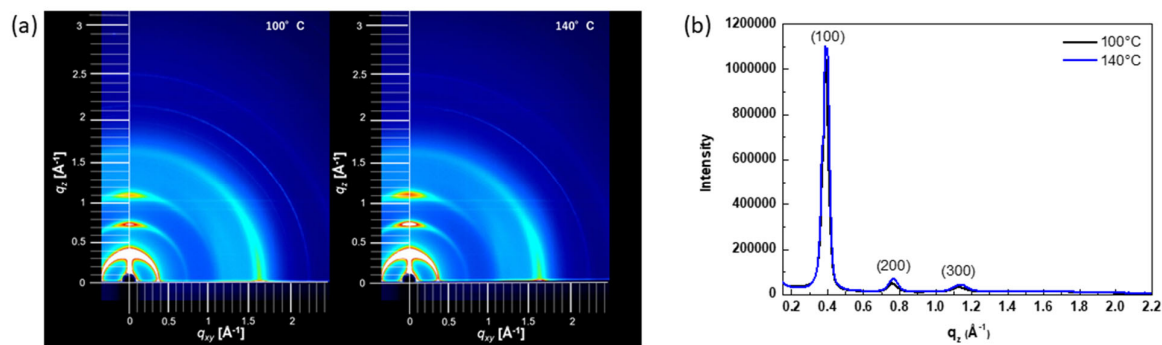

Figure S8: 2D-GIXRD patterns (a) and corresponding out of plane profiles (b) of P3HT layers as function of thermal annealing temperature.
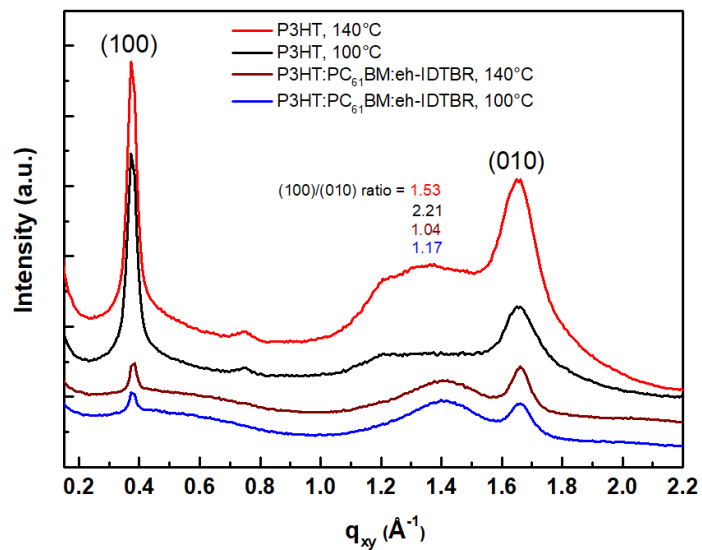
Figure S9: In plane profiles of P3HT and P3HT:PC$_{61}$BM:eh-IDTBR layers as function of thermal annealing temperature. Ratio of (100)/(010) peak intensities is given to evaluate the evolution ratio between edge-on and face-on orientation of P3HT polymer chain.